NBS REPORT

7241

Quarterly Report

for

December 1, 1961 to March 1, 1962

on

ELASTOMERIC SEALS AND MATERIALS

AT

CRYOGENIC TEMPERATURES

by

D. H. Weitzel, R. F. Robbins, Y. Ohori and P. R. Ludtke

U. S. DEPARTMENT OF COMMERCE
NATIONAL BUREAU OF STANDARDS
BOULDER LABORATORIES
Boulder, Colorado

THE NATIONAL BUREAU OF STANDARDS

Functions and Activities

The functions of the National Bureau of Standards are set forth in the Act of Congress, March 3, 1901, as amended by Congress in Public Law 619, 1950. These include the development and maintenance of the national standards of measurement and the provision of means and methods for making measurements consistent with these standards; the determination of physical constants and properties of materials; the development of methods and instruments for testing materials, devices, and structures; advisory services to government agencies on scientific and technical problems; invention and development of devices to serve special needs of the Government; and the development of standard practices, codes, and specifications. The work includes basic and applied research, development, engineering, instrumentation, testing, evaluation, calibration services, and various consultation and information services. Research projects are also performed for other government agencies when the work relates to and supplements the basic program of the Bureau or when the Bureau's unique competence is required. The scope of activities is suggested by the listing of divisions and sections on the inside of the back cover.

Publications

The results of the Bureau's research are published either in the Bureau's own series of publications or in the journals of professional and scientific societies. The Bureau itself publishes three periodicals available from the Government Printing Office: The Journal of Research, published in four separate sections, presents complete scientific and technical papers; the Technical News Bulletin presents summary and preliminary reports on work in progress; and Basic Radio Propagation Predictions provides data for determining the best frequencies to use for radio communications throughout the world. There are also five series of nonperiodical publications: Monographs, Applied Mathematics Series, Handbooks, Miscellaneous Publications, and Technical Notes.

A complete listing of the Bureau's publications can be found in National Bureau of Standards Circular 460, Publications of the National Bureau of Standards, 1901 to June 1947 ($1.25), and the Supplement to National Bureau of Standards Circular 460, July 1947 to June 1957 ($1.50), and Miscellaneous Publication 240, July 1957 to June 1960 (Includes Titles of Papers Published in Outside Journals 1950 to 1959) ($2.25); available from the Superintendent of Documents, Government Printing Office, Washington 25, D. C.

NATIONAL BUREAU OF STANDARDS REPORT

NBS PROJECT

NBS REPORT

81429

April 1, 1962

7241

ASD 33(616) 61-04

Quarterly Report

for

December 1, 1961 to March 1, 1962

on

ELASTOMERIC SEALS AND MATERIALS

AT

CRYOGENIC TEMPERATURES

by

D. H. Weitzel, R. F. Robbins, Y. Ohori, and P. R. Ludtke

<NBS>

U. S. DEPARTMENT OF COMMERCE
NATIONAL BUREAU OF STANDARDS
BOULDER LABORATORIES
Boulder, Colorado

IMPORTANT NOTICE

FOREWORD

This report was prepared by the National Bureau of Standards under USAF Contract No. 33(616)-61-04. This contract was initiated under Project No. 7340, "Nonmetallic and Composite Materials", Task No. 73405. "Elastomeric and Compliant Materials". The work was administered under the direction of Directorate of Materials and Processes, Deputy for Technology, Aeronautical Systems Division, with Mr. Roger Headrick acting as Project Engineer.

Program Status

The study of elastomeric seals at cryogenic temperatures has moved through the stages of initial development and functional testing[1] into a more analytical and fundamental program. At present the program consists of four experiments, one of which involves the direct measure of leak rate through a seal. The other experiments are designed to study the low temperature behavior of elastomeric polymers in terms of thermal expansion, resilience, force-temperature relationships, and differential thermal analysis. O-rings and test samples are prepared and supplied by the Elastomers and Coatings Branch of Materials Central, Aeronautical Systems Division.

1. Force Evaluation Experiment (P. R. L. and D. H. W.)
1.1 Introduction and Procedure

The purpose of this experiment is to measure the force on an o-ring while it is compressed and held at constant thickness during cooldown from room temperature to 76°K. The o-ring functions as a seal during the experiment, and the force and temperature at which a leak begins is noted. In addition, the force-temperature curve is continuously recorded so that not only the endpoints but the shapes of the curves for various elastomers can be compared.

The test apparatus is shown in Figure 1. The plates and bolts are overdesigned to minimize flexing or stretching which would place a spring load on the o-ring. Springloading will "smooth out" the force-temperature curve and help to maintain a seal in practical applications, but more meaningful comparisons of the various elastomers can be obtained in this experiment if springloading is minimized or eliminated.

In previous attempts to make these measurements[1] it was found that differences in cooling rates of various parts of the test jig caused force variations as high as 8000 pounds when the jig was cooled without an o-ring in position. This "differential contraction" problem was minimized by making all of the stressed parts of the jig of invar. This includes force washer sleeves, top plate, studs, and compression disc. Invar pillars are placed adjacent to the studs between the base and top plate to maintain a constant separation between these surfaces at all times. The invar pillars also keep the top plate and base accurately parallel, which insures uniform compression of the o-ring. The invar and pillar modification has made negligible the errors due to "differential contraction".

4

TO WHEATSTONE
BRIDGE CIRCUIT

VENT

TO LEAK
DETECTOR

LIQUID N₂

STAINLESS STEEL
TUBES

VACUUM
SPACE

LOADED FORCE
WASHER

PILLAR

MICA
INSULATION

LIQUID
N₂

LOADING
SLEEVES

TEMPERATURE
COMPENSATING
FORCE WASHER

THERMO-
COUPLE
LEADS
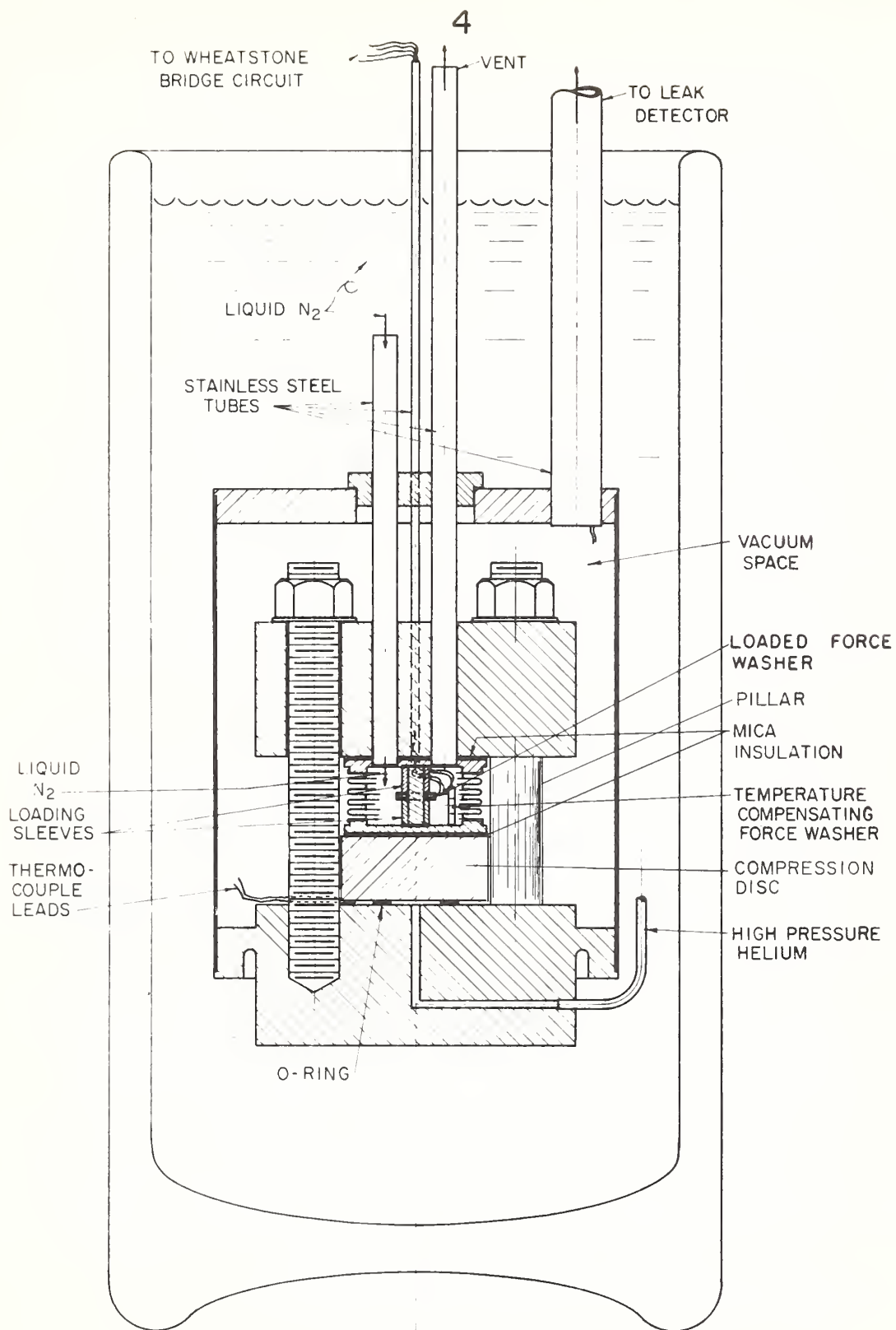
COMPRESSION
DISC

HIGH PRESSURE
HELIUM

O-RING

Figure 1. Force – Temperature   Test
Apparatus

The bellows assembly contains four washer type strain gauges. Three of these are loaded and the fourth is for temperature compensation. Liquid nitrogen is circulated through the bellows to maintain the force washers at constant temperature and to slowly cool the apparatus. It is only at the end of the cooldown period that liquid nitrogen is allowed to cover the entire test fixture. A thermocouple placed near the o-ring provides a record of o-ring temperature. The force washers and two external fixed resistors make a bridge circuit which provides a signal proportional to the force on the o-ring. The force and temperature signals are continuously plotted by an x, y recorder as the experiment progresses.

By varying the number of mica shims between the compression disk and the bellows, the 0.140 inch thick by 1 inch I.D. o-ring is compressed to an initial force of 14,000 to 18,000 pounds when the plates are pulled solidly down on the invar pillars. After this initial compression the outer cover is soldered to the base of the jig. During soldering the o-ring is warmed to around 40°C, which accelerates relaxation of the elastomer. After cooling to room temperature the force is again measured before introducing helium pressure and starting to cool with liquid nitrogen.

1.2   Results and Discussion

Meaningful results have thus far been obtained for three different polymers supplied by ASD. These are natural rubber (IV-8A)*, ethylene propylene rubber (IV-29C), and cis-4 polybutadiene (IV-29B). The force-temperature curves and other pertinent information for these materials are shown in Figures 2, 3, and 4, and the results are summarized in Table 1.

The ethylene propylene (IV-29C, Figure 2) o-ring was compressed to .018 in. thickness (87% compression) which required an initial force of 13,900 pounds. After soldering and relaxing overnight the force had decayed to 11,000 pounds. The first cooldown was carried out with 100 psig of helium gas inside the seal. At 196°K the force had fallen to about 5,800 pounds and the seal began to leak. After warm-up the test was repeated with the same pressure inside the o-ring and a leak began at 208°K. Note that the second curve falls to the left of the first, indicating a relaxation of 500 to 1000 pounds in the

---

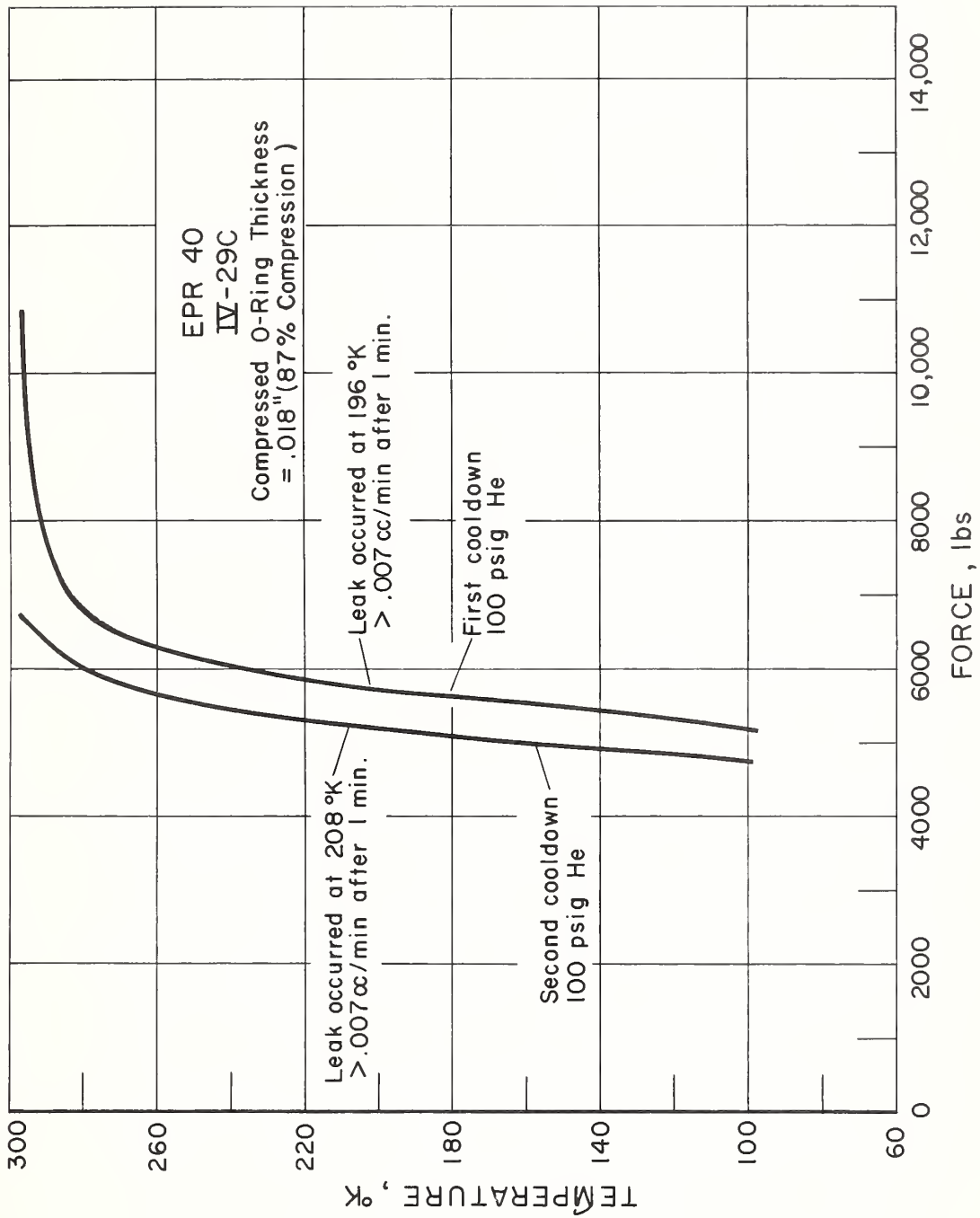* Compounding recipes are given in the Appendix.

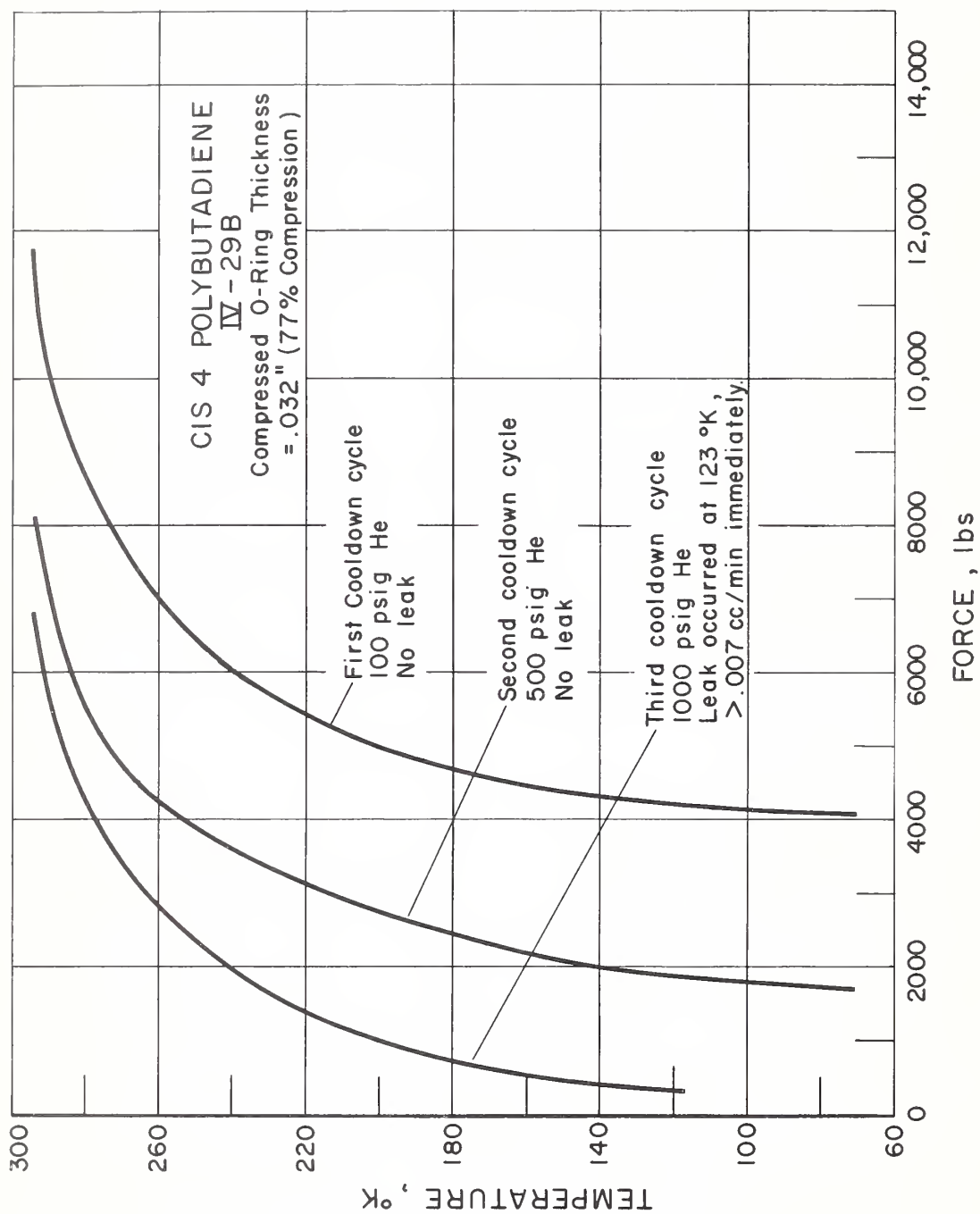Figure 2. Force – Temperature Curve, Ethylene Propylene Rubber

7

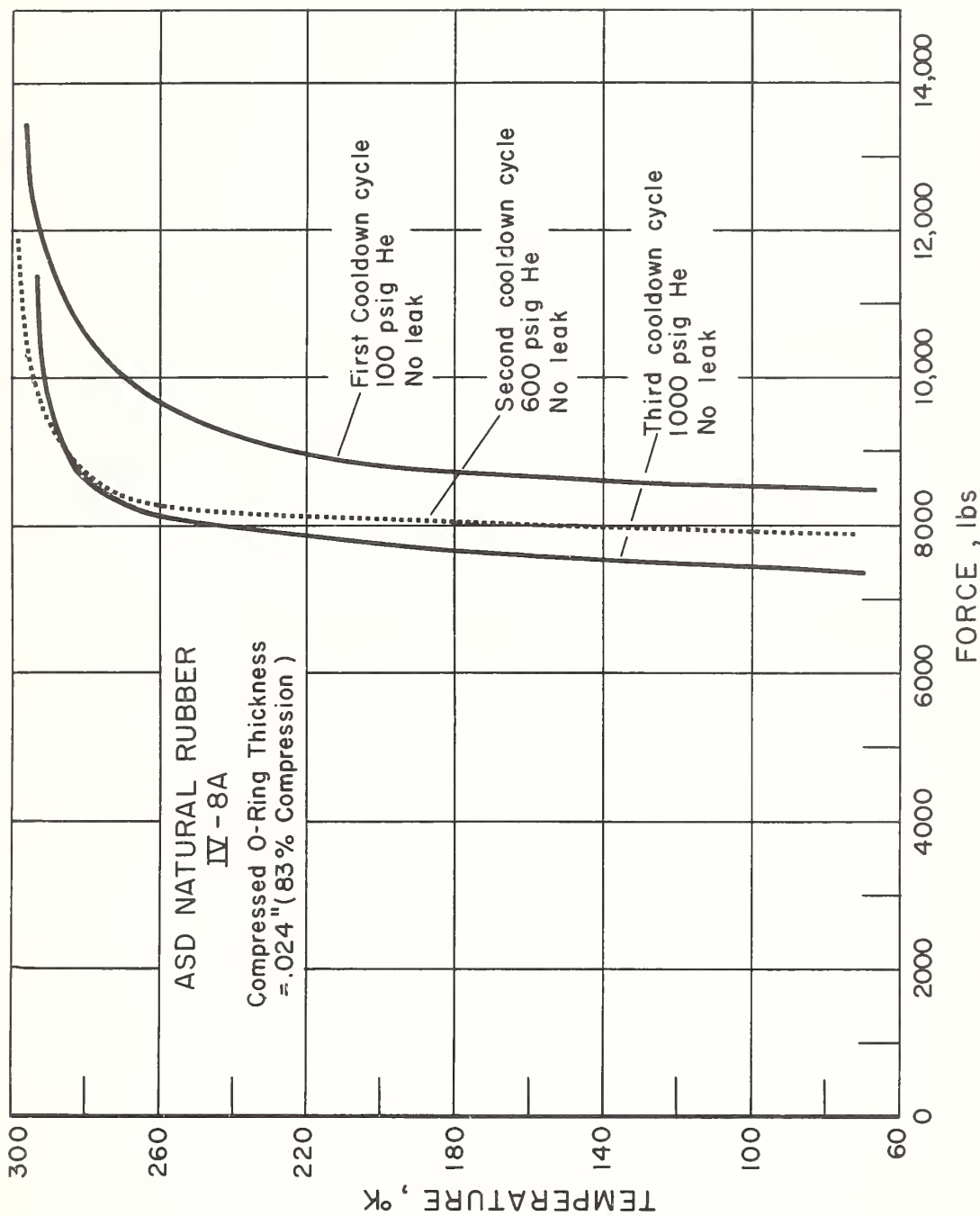Figure 3. Force – Temperature Curve, Cis – 4 Polybutadiene

Figure 4. Force-Temperature Curve, Natural Rubber

| Polymer | Compound Number | Shore A Hardness | Initial Force (lbs.) | Force After Initial Relaxation | Force Lost During Initial Relaxation | Force at Start of Cooldown | | | Compressed O-Ring Thickness | Compression | Material Failure | Leak Occured | | | |
						#1	#2	#3				Temp.	Force	He Press. (psig)	Off Scale Time
EPR-40	IV-29C	60	14,000	11,000	21%	11,000	9,000	8,800	.018"	87%	None	196°K	5800	100	1 Min.
Cis-4 Polybuta-diene	IV-29B	70	14,000	11,500	19%	11,500	8,000	7,500	.032"	77%	None	123°K	400	1000	1 Sec.
Natural Rubber	IV-8A	65	18,000	13,000	26%	13,000	12,000	12,000	.024"	83%	None	76°K*	7400	1250	1 Sec.

* A leak occurred when the test jig was removed from the liquid nitrogen bath and set down on the concrete floor.

Table 1. Force Evaluation Test Data

force on the o-ring.

The initial force of about 14,000 pounds required to compress the o-ring 87% is somewhat misleading because of the way it is applied. In order to adjust the force it is necessary to remove or add mica shims between the bellows and the plates. This results in several cycles of loading and unloading which "condition" the o-ring and cause it to take a certain amount of compression set. The final force required for "initial" compression is consequently lower than it would be if the o-ring were compressed only once to its final thickness and held there. The difference between these two methods of compression for o-rings of the size used here can be several thousand pounds. This must be kept in mind when designing flanges for a seal of this kind.

Compound IV-29C is relatively soft, having a Shore A durometer reading of 60, and also seems to exhibit a relatively low friction coefficient. When compressed with a high force the o-ring tends to flow and extrude outward, making it difficult to confine between flat flanges and allowing the initial force to decay rapidly. In spite of this the o-ring showed no sign of material failure after the test. A new compound of this material having somewhat higher durometer should be prepared for further testing.

Figure 3 gives results for an o-ring of cis-4 polybutadiene (ASD sample IV-29B) which was compressed to .032" (77% compression), requiring an initial force of 14,200 pounds which had relaxed to 11,500 pounds when cooldwon was begun. During the first cooldown, with 100 psig He in the seal, the force decayed to 4000 pounds and during the second cooldown, with 500 psig, the force fell to about 1700 pounds. In both cases there was no leak. During the third cooldown, with 1000 psig inside the o-ring, a leak ocurred at 123°K after the force had decayed to less than 500 pounds. Since the gas pressure on the flange area inside the compressed o-ring would account for most of this force it appears that the compression on the o-ring when it leaked was almost zero. One might expect this to always be the case, but many of the o-rings begin to leak while the total flange load is still quite high. Evidently small leak passages can occur with some of the elastomers even though most of the sealing surface is still held under high load against the flanges. This may indicate some irregularity or non-uniformity in the way the highly compressed material contracts when it is cooled. At any rate it is surprising and interesting to see how well the cis-4 polybutadiene held a seal in spite of its high rate

of force decay and the large amount of relaxation between tests. A slightly higher initial compression would probably have maintained the seal through all three test cycles.

The natural rubber o-ring (sample IV-8A, Figure 4) was compressed 83%, to a thickness of .024 inches, which required a force of 17,800 pounds. This had relaxed to 13,000 pounds at the beginning of the test. Cooldowns were carried out with 100, 500, and 1000 psig helium inside the seal. No leak ocurred. At the end of the 1000 psig cooldown, with the seal at 76°K, the pressure was increased to 1250 psig. No leak ocurred, but when the apparatus was removed from the bath and lightly jarred on the concrete floor a leak began.

One general observation in all of these tests is the absence of any significant change in the force-temperature curves as the elastomer passes through the brittle point transition temperature (Tg). It was expected that there would be a definite increase in the rate of force decay at Tg, where the material would normally begin to contract as a rigid solid. Possibly the high compression, close confinement due to friction, and low final thickness combine to prevent the material from showing any sudden change as it passes through the transition temperature.

Force-temperature curves for additional ASD materials will be presented and compared in subsequent reports.

2.   Thermal Expansion (Y. O. and R. F. R.)

2.1   Introduction

During the reporting period the thermal expansions of the isobutylene-isoprene co-polymers (Group III) and two additional co-polymers have been tested. These results, along with those previously reported, have been divided into groups of similar materials and plotted in Figures 5, 6, and 7.

As the information concerning low temperature expansions becomes more complete, correlation of the experimental results with various theories should be investigated. Accordingly, two relations correlating the glassy state transition temperature (Tg) of a co-polymer with the Tg's of the corresponding homopolymers will be discussed. In addition a relation between the expansivities above and below Tg will be presented. Discussion of the thermal expansion mechanism which was touched on in our last report [1] will be continued, with particular
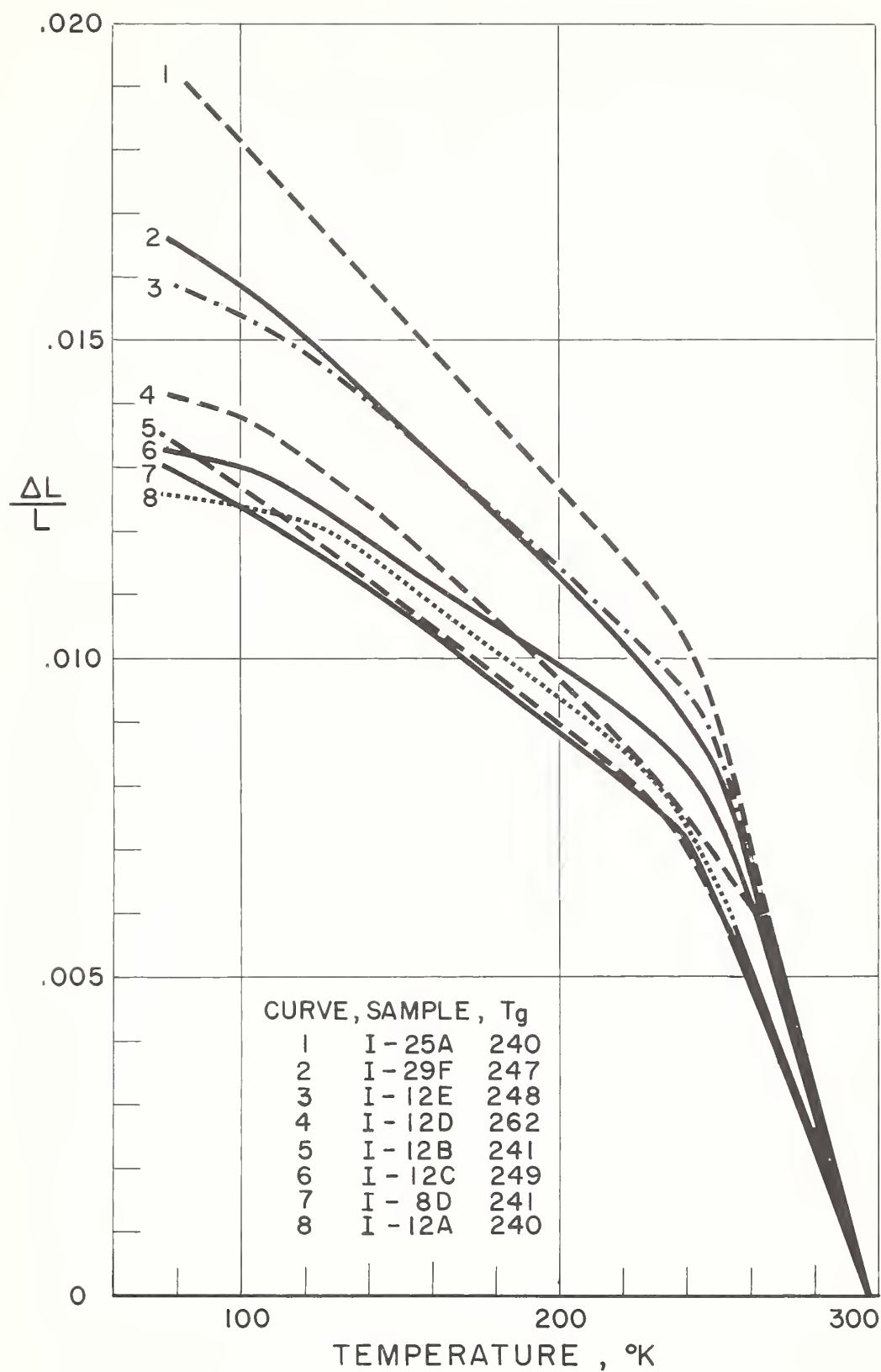
12

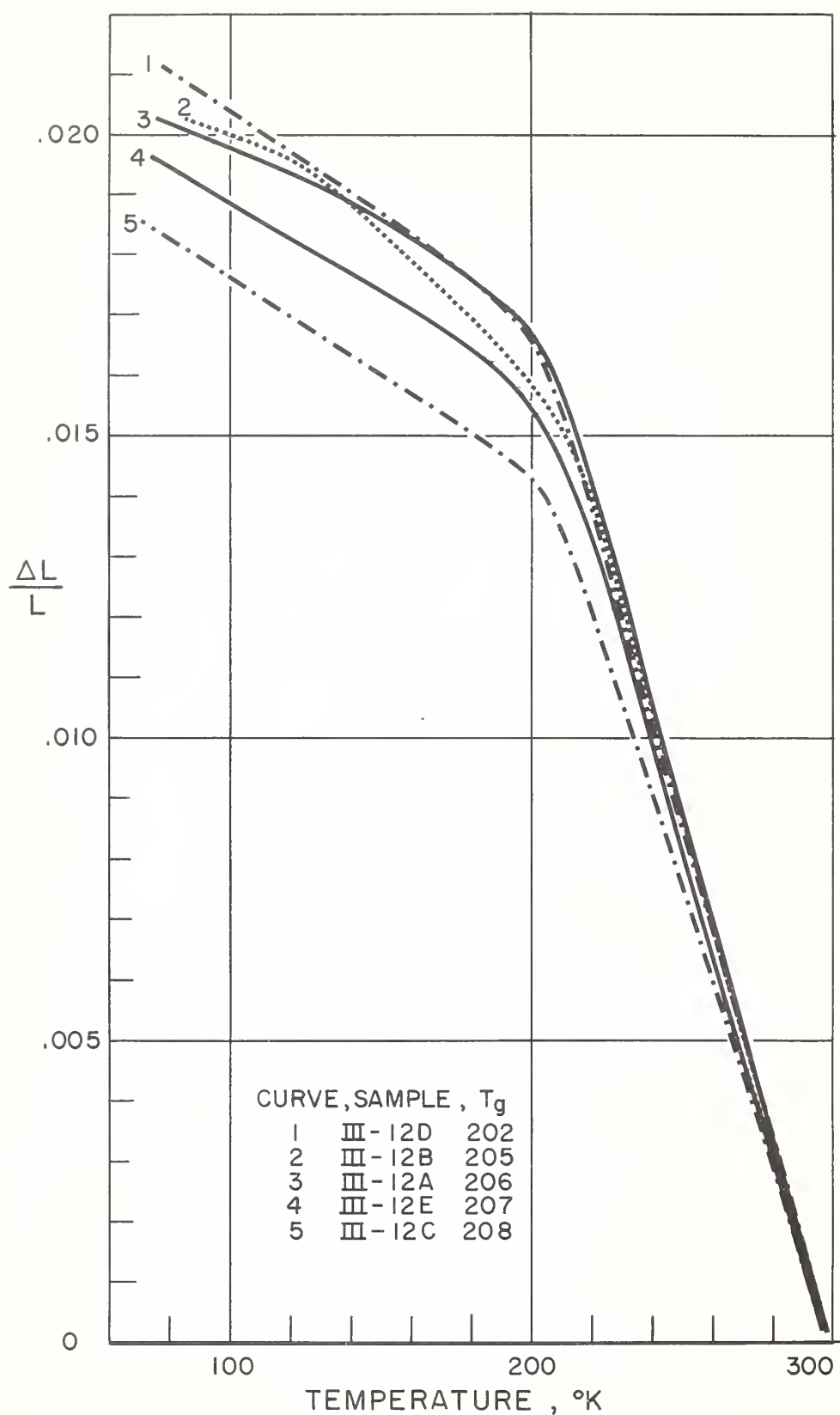Figure 5. Thermal Expansion and T_G, Group I

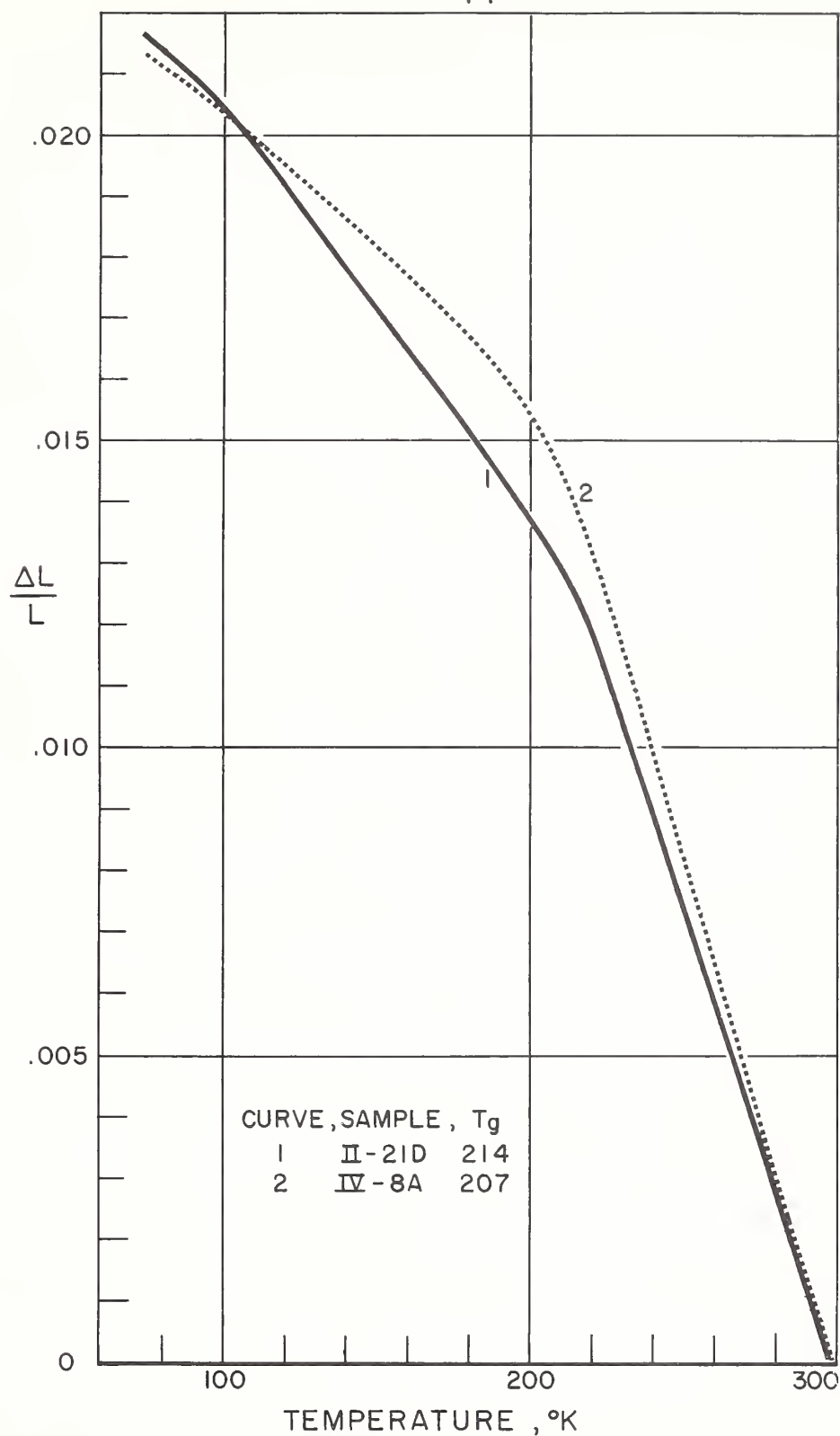Figure 6. Thermal Expansion and T_G, Group III

14

Figure 7. Thermal Expansion and
T_G, Group II and IV

attention given to time phenomena.

2.2   Thermal Expansion Mechanisms

It is widely accepted that there are two distinct mechanisms responsible for the contraction of an elastomer while the temperature is being reduced, and that the effect of one of these mechanisms becomes very small near and below Tg. The first mechanism is the familiar thermal vibrational change in amplitude of the atoms. For the second mechanism there are several possible interpretations. [2, 3, 4, 5]. Two of these will be discussed at this time.

First we will consider the "diffusion of holes" theory advanced by Alfrey, et al,[3] and others. The elasticity of rubber-like materials is made possible by the random orientation of long molecular chains which are tangled with one another, and joined occassionally by chemical bonds. Such an imperfect packing requires that there be certain gaps or "holes" in the structure[6]. When these materials cool, the structure becomes more packed and tends toward a more ordered state, causing the equilibrium volume of the holes, and hence the free volume, to decrease. However, this volume contraction cannot take place instantaneously since the molecules must move to a new position. The molecular re-orientation cannot affect the "true" volume of the sample; it can only redistribute the holes, which will combine or divide in a random fashion. A consequence of this diffusion of holes is that if the material is to contract, some of the holes must diffuse to the surface of the sample and disappear[4].

At temperatures above the Tg range the time necessary to attain an equilibrium free volume is much faster than normal experimental times. Near Tg the equilibrium time required approaches the experimental time, and below Tg the holes are essentially "frozen in", and the material is unable to reach its equilibrium structure within a reasonable length of time. Hence the sharp change of slope of thermal expansion curves around Tg. Some contraction still takes place, due to the change in the amplitude of anharmonic vibrations with temperature. This vibrational effect is present throughout the temperature range, but is predominant only below Tg.

Next let us consider the concept of free rotation about carbon-carbon bonds, to be compared with the time effect considerations of hole diffusion. Tg was inferentially defined above as the temperature where the time required to attain the equilibrium free volume was equal

to the time of the experimental observation. Tg can also be defined as the temperature where the free rotations of C-C bonds ceases[3, 8]. The viscous flow mechanism for polymer transitions as advanced by Boyer and Spencer[4] is in accord with the concept of free rotation, and will be discussed briefly.

Consider several long chain molecular segments placed side by side, and the contraction of these molecules when the material is cooled. Perpendicular to the chains, contraction would be caused by decreased vibration of the molecules, and should obey normal laws which predict a linear variation with temperature. Contraction parallel to the segments, however, would have to be caused by other mechanisms, since changes in primary bond distance or valence angle are unlikely[8]. The mechanism suggested here is that contraction in the parallel direction of the over-simplified model is caused by displacement of entire chains relative to one another, in a manner similar to viscous flow. The net result of the flow of the molecules would be a contraction with decreasing temperature which is time dependent. Since free rotation is a requirement for viscous flow, this effect would not appear below Tg.

In samples randomly oriented, such as the polymers tested in this program, the length changes parallel and perpendicular to the chains would be superimposed on one another, and entanglements would inhibit the movements. However, since length-wise movement is zero below Tg, this theory predicts a change in slope of the expansion curve at Tg in agreement with known results. This theory also predicts differences in the expansivities of oriented samples measured in different directions, a result which has been verified experimentally[4]. Another obvious prediction is that if a rubber-like material at room temperature could be oriented so that the chains were mostly parallel to the direction of compressive force, contraction below Tg could be reduced to near zero in an o-ring seal application.

2.3   Experimental Results

The dilatometer used for the thermal expansion measurements has already been described[1]. Figures 5, 6, and 7 show the results which have thus far been obtained in our program. Each curve has been repeated at least once; in cases where the tests on a given material were not in good agreement, more runs were required to insure the reporting of reliable data. Useful numbers derived from the curves, such as the average coefficients of expansion above and below Tg, are

presented in Table 2.

It is interesting to compare curves 2 and 7 of Figure 5. The base polymers for these are identical; however, the polymer for curve 7 contains 25 parts of carbon black while that for curve 2 contains no carbon black. Both contain 20 parts of magnesium oxide. If curve 2 is taken as the additive expansion of the pure polymer and 16.5% (20 parts) magnesium oxide, the overall contraction from 300°K to 76°K for the carbon filled elastomer can be estimated. The calculated value obtained in this way is about 7% higher than the experimental.

The curves plotted in Figure 6 show various isobutylene/isoprene co-polymers compounded in approximately the same manner. It can be seen that compound III-12C has the minimum overall contraction, due to a lower coefficient of expansion above Tg. Compound III-12B seems to have a larger, more irregular contraction below Tg than the others. In future work, more emphasis will be placed on groups II, IV, and V.

2.4 A Relation Between Linear Expansion Coefficients α_g and α_r

In section 2.2 it was suggested that viscous flow plays an important part in thermal expansion, and that below Tg the free volume of a sample is constant. It has also been postulated that Tg for various polymers is a state of constant fractional free volume. These considerations can be related by considering the relation between viscosity, Tg, and fractional free volume, as proposed by Williams, et al,[9] and expanded by Tobolsky[10].

$$\log \frac{\eta(T)}{\eta(Tg)} = \frac{1}{2.303} \left(\frac{1}{f} - \frac{1}{fg} \right) \tag{1}$$

where

$\eta(T)$ is the viscosity at temperature T

$\eta(T_g)$ is the viscosity at temperature Tg

f is the fractional free volume at T

fg is the fractional free volume at Tg.

18

Sample	T_g (°K) Theoretical Eq. (7)	Eq. (6)	Experimental	α_r (°K⁻¹)	α_G (°K⁻¹)	a_2 (°K⁻¹)	$\frac{\Delta L}{L}$ from 297°K to 76°K
I-8D	242	247	241	1.3×10^{-4}	$.36 \times 10^{-4}$	3.3×10^{-4}	1.29×10^{-2}
I-29F	242	247	247	1.8	.48	4.0	1.65
I-12B	242	247	241	1.3	.36	2.7	1.35
I-12A	---	---	240	1.4	.36	3.0	1.26
I-12D	264	270	262	1.9	.45	4.5	1.41
I-12E	250	254	248	1.9	.45	4.5	1.58
I-25A	250	254	240	1.9	.55	3.9	1.94
I-12C	242	247	249	1.8	.33	4.5	1.32
II-21D	213	212	214	1.6	.68	2.8	2.15
III-12C	203	203	208	1.6	.54	3.2	1.84
III-12E	203	203	207	1.8	.29	4.5	1.94
III-12D	203	203	202	1.7	.36	3.9	2.11
III-12A	---	---	206	1.9	.28	4.8	2.02
III-12B	203	203	205	1.7	.38	3.9	2.02
IV-8A	---	---	207	1.7	.51	3.6	2.14

Table 2. Summary of Thermal Expansion and Tg Results

The dependence of free volume on temperature is taken to be the difference between the volume expansion coefficients a_r and a_g, where subscripts r and g refer to the "rubbery" and "glassy" states of the polymer. Then

$$f = f_g + (a_r - a_g)(T - Tg) = f_g + a_2 (T-Tg) \tag{2}$$

Combining (1) with (2), we obtain:

$$\log \frac{\eta(T)}{\eta(Tg)} = \frac{-1}{2.303 \, f_g} \left(\frac{T - Tg}{f_g / a_2 + T - Tg} \right) \tag{3}$$

Experimental data [11] have established the validity of the following emperical relation:

$$\log \frac{\eta(T)}{\eta(Tg)} = - \frac{17.44 \, (T-Tg)}{51.6 + T - Tg} \tag{4}$$

Equating the constants of (3) and (4), we can determine constant values for f_g and a_2, as follows:

$$f_g = 0.025$$

$$a_2 = a_r - a_g = 4.8 \times 10^{-4} \, \deg^{-1}$$

The above development, together with experimental verification of equation (4), are the best evidence that f_g is essentially constant for all polymers, and that the difference $a_r - a_g$ should be constant. If we assume isotropic contraction, $a \approx 3\alpha$, and

$$a_2 \approx 3 (\alpha_r - \alpha_g) \tag{5}$$

where α_r is the "rubbery" coefficient, and α_g is the "glassy" coefficient.

In Table 2 values of a_2 are approximated from α_r and α_g, and are found to be in the range of 2.7 to 4.8 x 10^{-4} deg $^{-1}$, in general agreement with the above theory.

2.5 Two Relations Between Monomer Ratios and Tg

The value of Tg for an amorphous co-polymer can be estimated if the values of Tg of both homopolymers are known. One of the more widely used empirical formulas relating these is [12, 13]

$$\frac{1}{Tg} = \frac{W_1}{Tg_1} + \frac{W_2}{Tg_2} \tag{6}$$

where Tg_1 and Tg_2 apply to the homopolymers and W_1 and W_2 are their respective weight fractions. In some cases, the following formula has been found to be more accurate [14]:

$$Tg = x_1 Tg_1 + x_2 Tg_2 \tag{7}$$

Here x_1 and x_2 are the mole fractions of the homopolymers.

Table 2 shows the values of Tg calculated by equations 6 and 7, and the experimental Tg obtained by extrapolating straight line portions of the expansions below and above Tg, using the intersection as Tg. Values of Tg for the homopolymers were obtained from published data [15]. The experimental and calculated results are in good agreement, indicating that equations 6 and 7 can be applied to predict values of Tg for new materials which might have applications at low temperature.

3.   Resilience (D. H. W.)
3. 1   Introduction

The elastic response of a given rubber-like material is determined primarily by time and temperature.   The capacity for storing and returning energy in a rapid deformation is called resilience.   A simple form of rapid deformation results when a rubber ball is dropped on a hard surface.   Alternately, a flat rubber sample can be deformed by a striker which is free to rebound with energy returned by the rubber.

Resilience has the attractive feature of being intimately associated with the structure of the molecule and the nature of the intermolecular forces rather than the gross structure of the material [17].   The temperature of minimum resilience is closely correlated with the second order transition temperature (T_g) and usually occurs 15° to 20°C above this point.   The incorporation of a plasticizer lowers both T_g and the temperature of minimum resilience; the addition of carbon black has the effect of broadening the temperature resilience curve without affecting the position of the minimum [18].

Since resilience is a dynamic property demonstrated by rapid deformation and recovery it is not readily associated with o-ring seal performance.   That there will be no correlation between cryogenic seal performance and low temperature resilience may, however, be a premature conclusion.   Natural rubber, for example, has a high coefficient of expansion and relatively low compression modulus. Both of these might lead one to expect poor performance as a seal at extreme low temperature but our tests have shown that natural rubber is actually one of the best elastomers for this application.   Its high resilience may be at least partly responsible.

The point of minimum resilience for various elastomers has been studied and interpreted by others[18] but we have not found any studies which carry the measurements or theory to extreme low temperatures.   These considerations, together with the simplicity of the resilience test and its close relation to molecular structure have led us to include it in our testing program.

3. 2   Experimental

Figure 8 shows the method which is being used to cool a stand-
ard cylindrical test button (1 square inch cross section by 1/2 inch
long) and obtain resilience values by visual observation of rebound
height of a 1/2 inch steel ball.   Temperature is measured and recorded
through use of a copper-constantan thermocouple.   The sample is held
firmly in position under moderate load provided by a copper ring and
flexible plate screwed to the top of the anvil.   This prevents motion
of the sample which might otherwise absorb some of the energy of the
striking ball.   Since the ball falls without friction other than air
resistance it is assumed that the rebound height is a fair measure of
the energy returned by the elastomer.   The resulting curve for
natural rubber (ASD sample No. IV-8A) is shown in Figure 9.

The resilience of natural rubber measured under these condi-
tions shows a high temperature maximum of 57% near 340°K, drops to
a minimum of 3% near 240°K, then rises sharply to about 70% at 210°K
and continues to increase with decreasing temperature until it levels
off at 90% when the temperature reaches 100°K.   Below 100°K the
resilience appears to be stable, but no measurements have been
obtained below 80°K.

Mullens[18] in 1946 reported a minimum resilience of 5% for
natural rubber at 238°K.   Since his equipment was entirely different
from ours and we have no knowledge of his compounding recipe, it
seems remarkable that our results should be in such close agreement.
We hope that this is not fortuitous, but instead points up the basic
nature of resilience as a property characteristic of the polymer.

Some modifications of our apparatus to eliminate the need for
an operator in constant attendance are under way.   These consist of a
clock-activated striker and an automatic record of rebound height
along with temperature.   This improved equipment should make it
possible for us to obtain resilience - temperature curves for many of
the ASD materials in a relatively short time.

4.   Differential Thermal Analysis (R. F. R.)
4. 1   Introduction

The differential thermal analysis (DTA) test program initiated
last fall has progressed to the point where some meaningful results
may be reported.   DTA curves for four materials in Group IV and one
in Group V have been obtained.   In addition, a curve illustrating

Meter scale (Mirrored glass)

Guide tube

Magnet

½ Dia steel ball

Sliding plastic scale.

To Vacuum

Insulation

Sample

Thermocouple

Liquid N₂ dewar

Dewar

Cooling coil
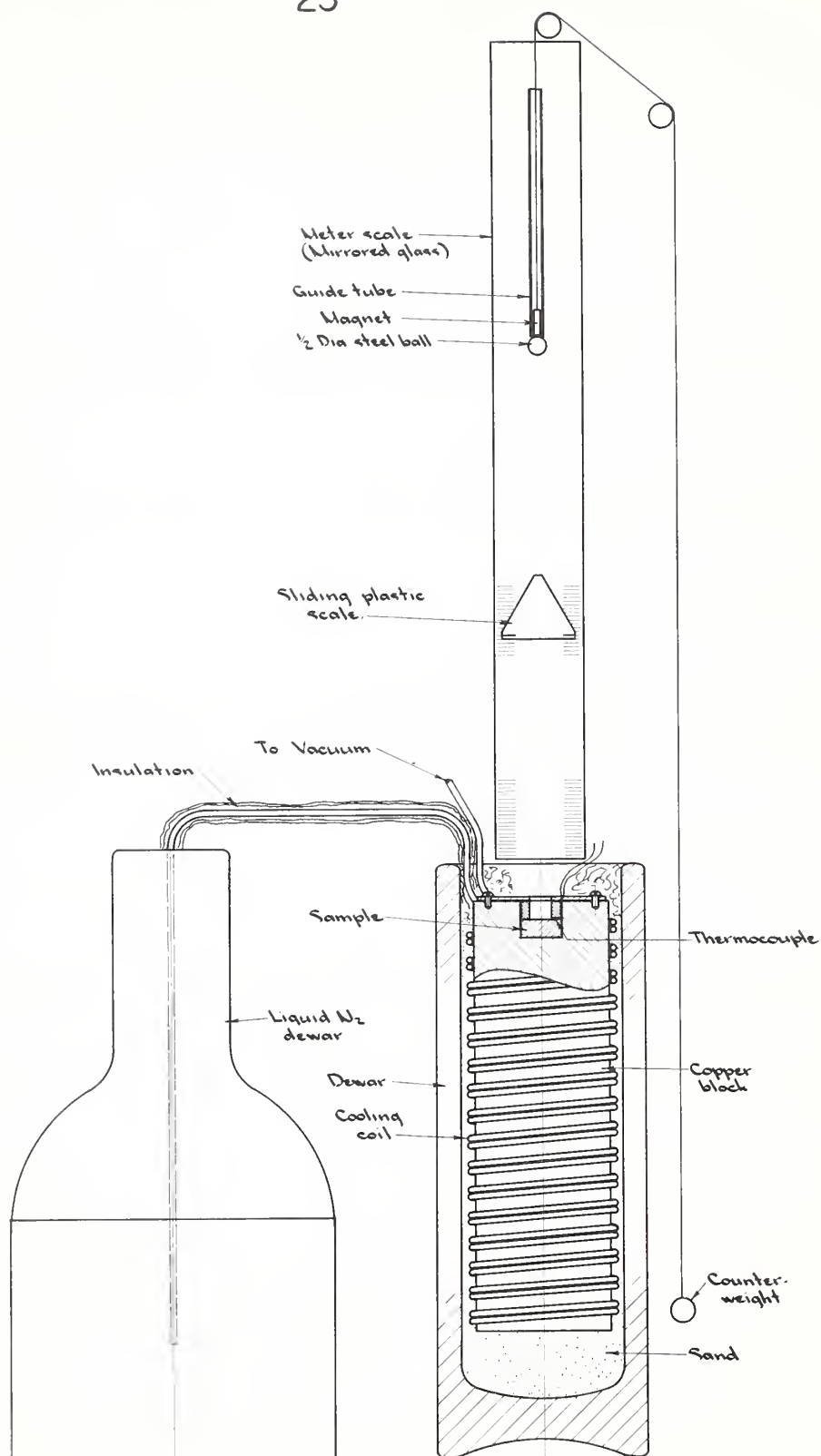
Copper block

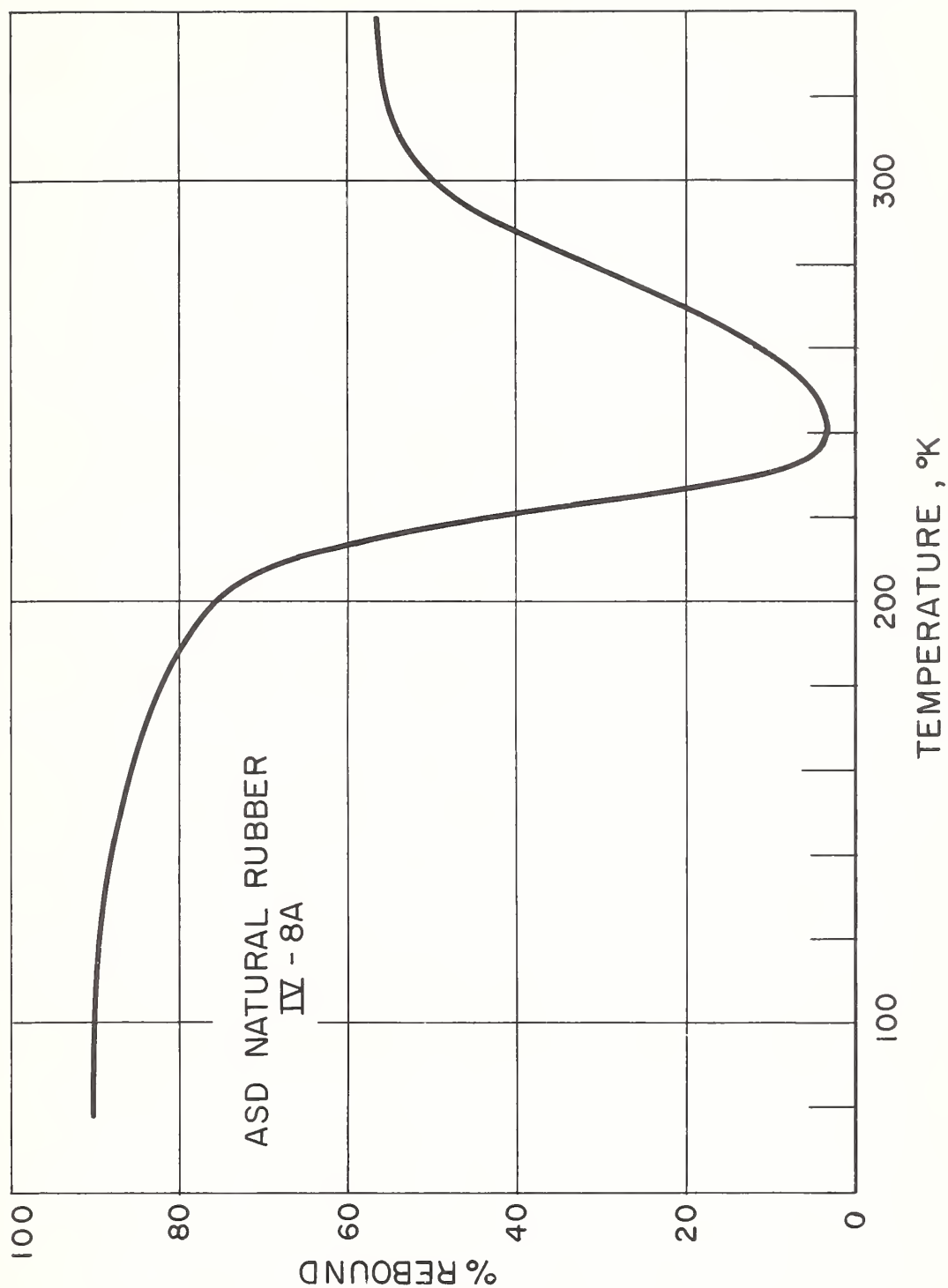Counter weight

Sand

FIGURE 8   - REBOUND RESILIENCE APPARATUS

Figure 9. Rebound Resilience of Natural Rubber

the interesting effect of a vacuum environment on a stable elastomer in Group I will be described.

4.2 Experimental Apparatus and Procedure

The experimental set-up used in tests conducted with a vacuum environment surrounding the sample has already been described[1]. Briefly, the apparatus consists of a copper can connected to a vacuum pumping system, and the appropriate instrumentation to measure the temperature difference from a point in the middle of the sample to a point near the surface. One half inch diameter by one half inch long solid cylindrical samples are used, and a reference sample is unnecessary. The vacuum can is lowered into a metal dewar and cooled to 76°K before each test. The curves are obtained during warm-up of the sample, which is surrounded by copper caps to insure uniform heating.

For tests without a vacuum space this dewar arrangement was found to be inadequate, since warming rates were too high. A glass 6 inch diameter dewar with 2 inches of additional expanded foam insulation inside allowed the sample to warm to 275°K in about 7 hours. This dewar was used during the tests shown in Figures 10 through 14.

Temperature versus time is continuously recorded by two strip chart recorders. To plot the resulting information, times are matched with temperature (T) and temperature difference (ΔE) to determine temperature intervals for the various events.

An x, y recorder was also used for a short period, plotting T vs ΔE directly. Such a method is simple, but does not yield information about the shape of the warming curve, which is rather important in the vacuum tests. The runs described in the next section employed the x, y recorder, since warming rates were known to follow a smooth curve.

4.3 Test Results in a Dry, Nitrogen Atmosphere

Figures 10 through 15 show DTA curves plotted from data continuously recorded on the x-y recorder. As many as three tests were made on some samples to determine the reproducibility of the results. It can be seen that the shape of the curves and the events are reproducible, but the level of temperature difference varies due to variation in the warming rate. This can be due to several inherent
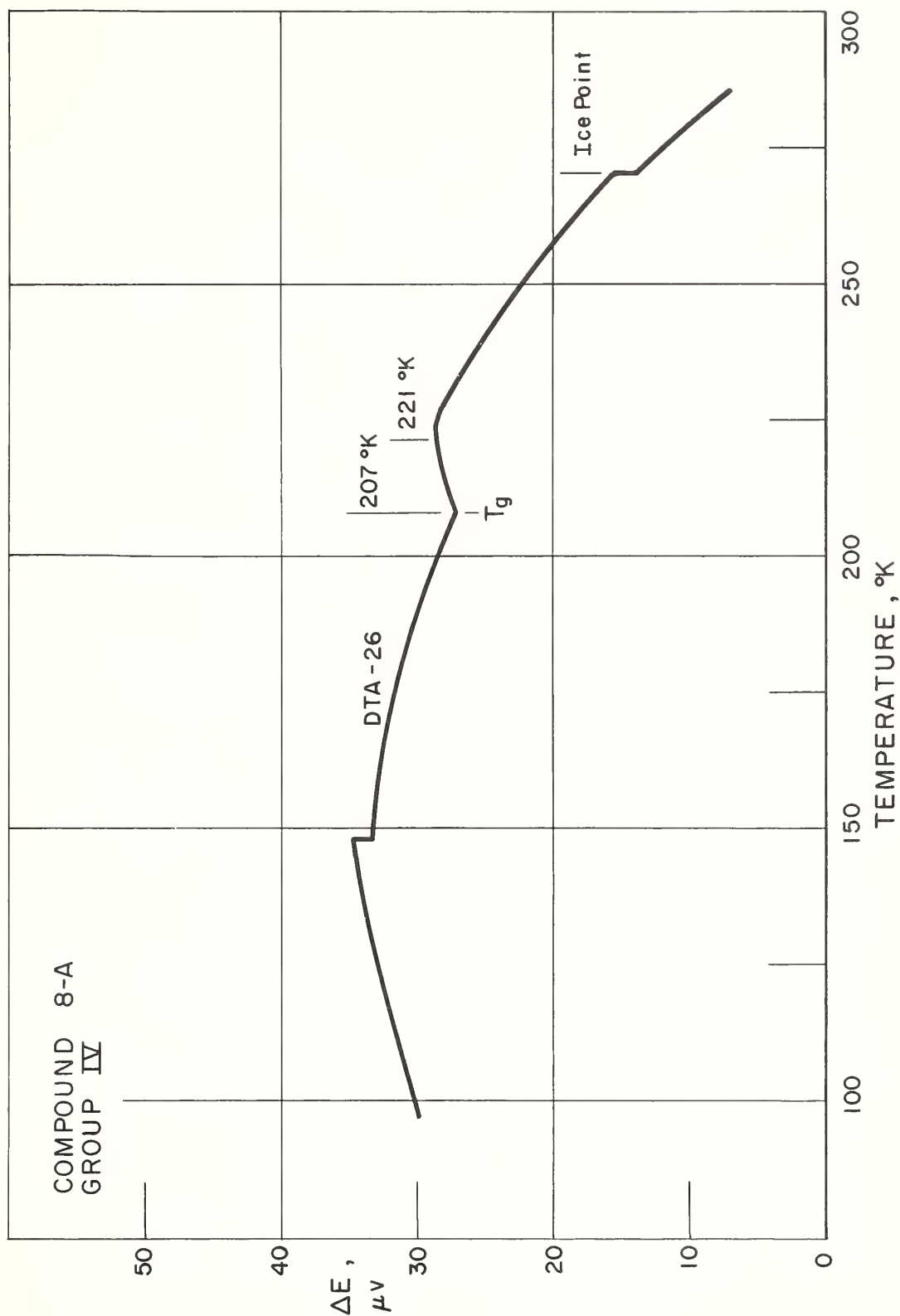
Figure 10. DTA Results, Compound IV - 8A

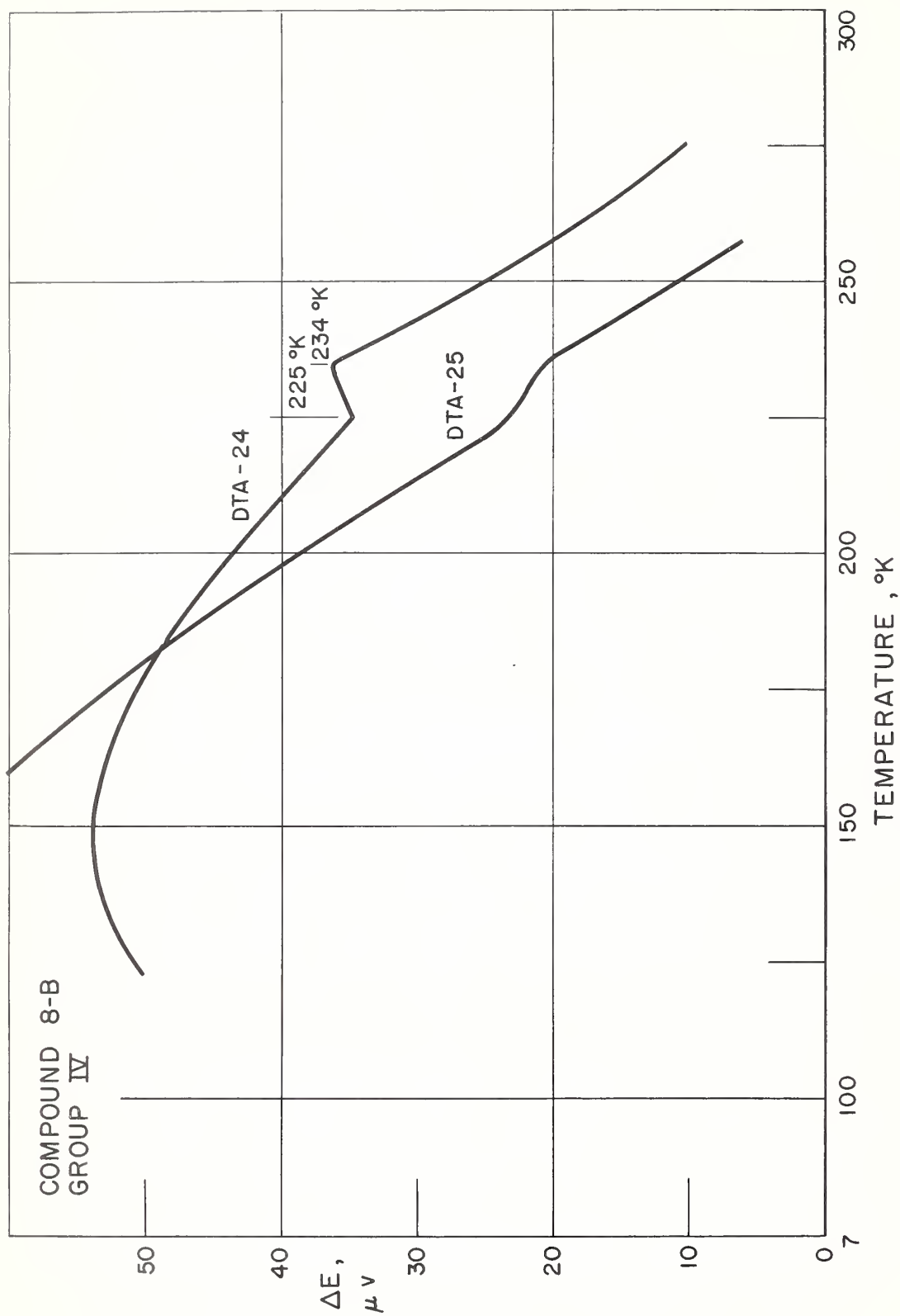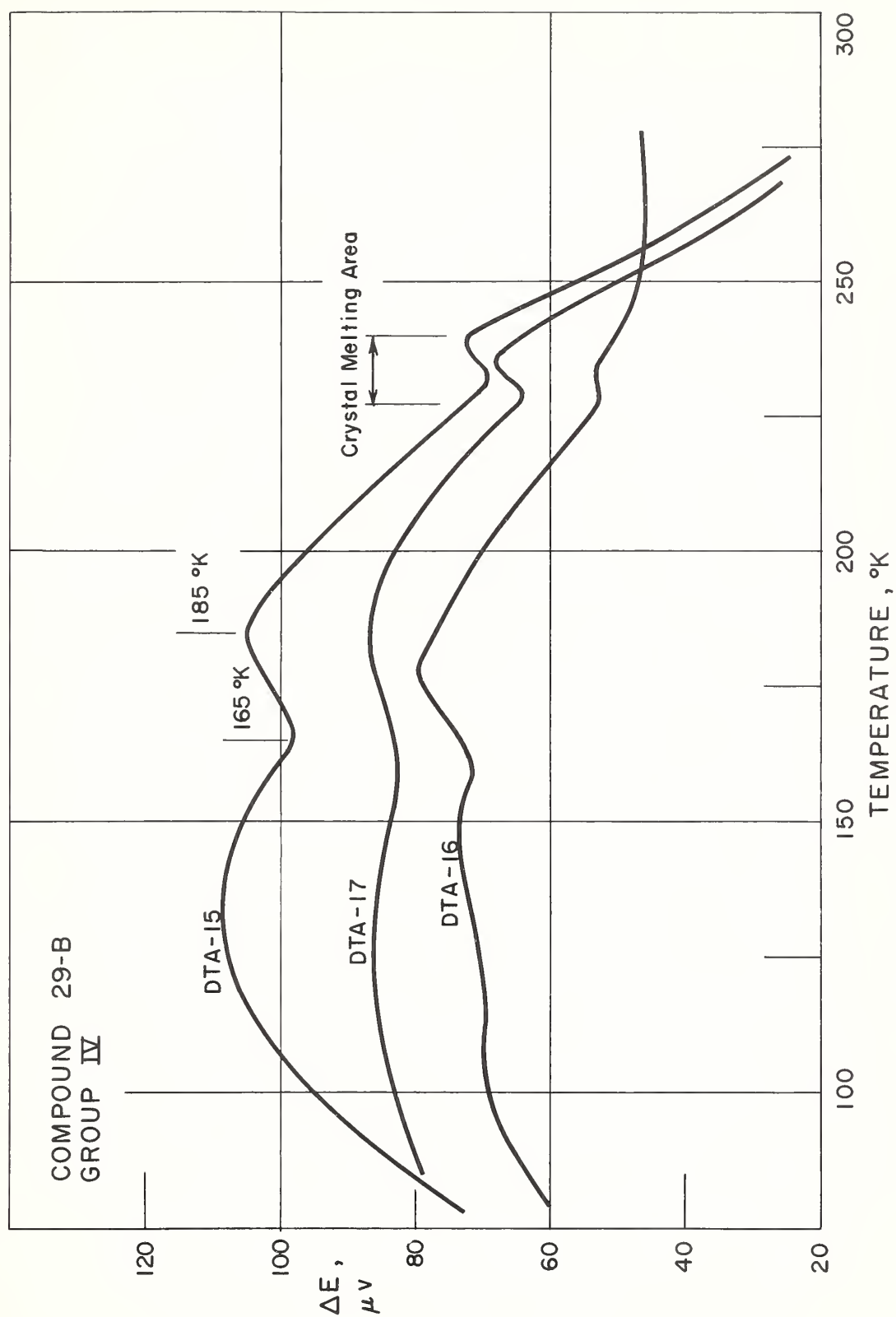Figure II. DTA Results, Compound IV - 8B
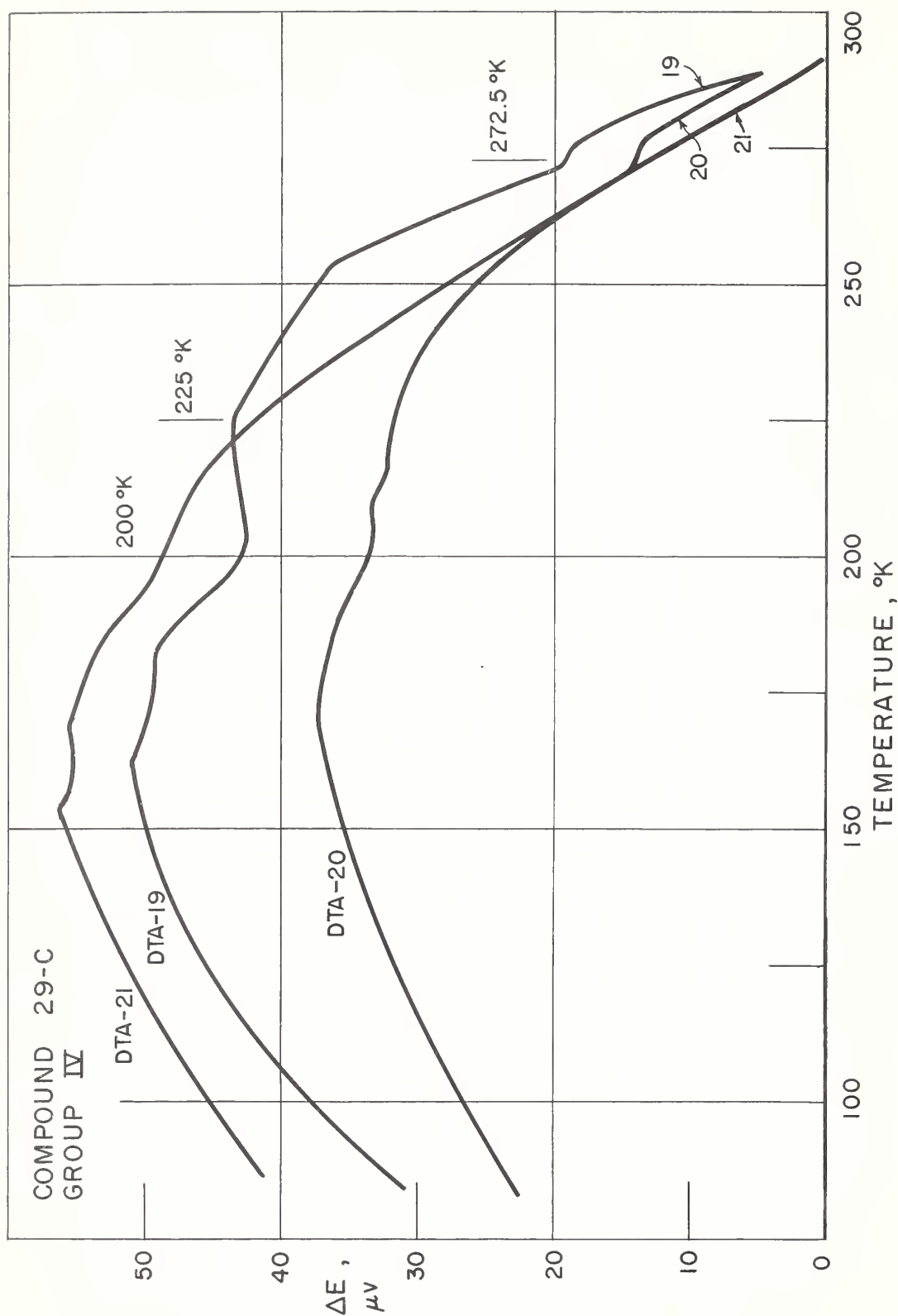
Figure 12. DTA Results, Compound IV - 29B

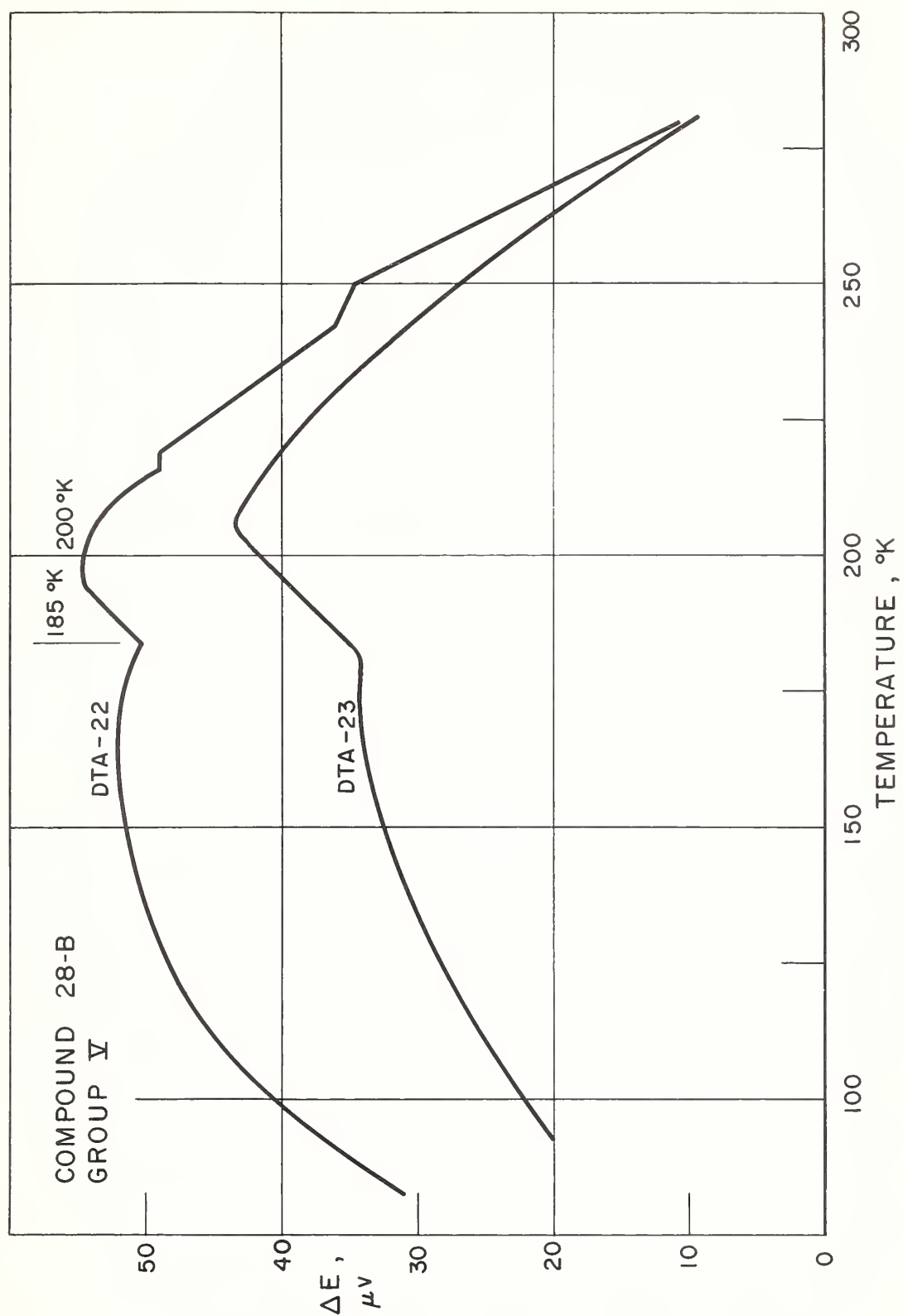Figure 13. DTA Results, Compound IV - 29C
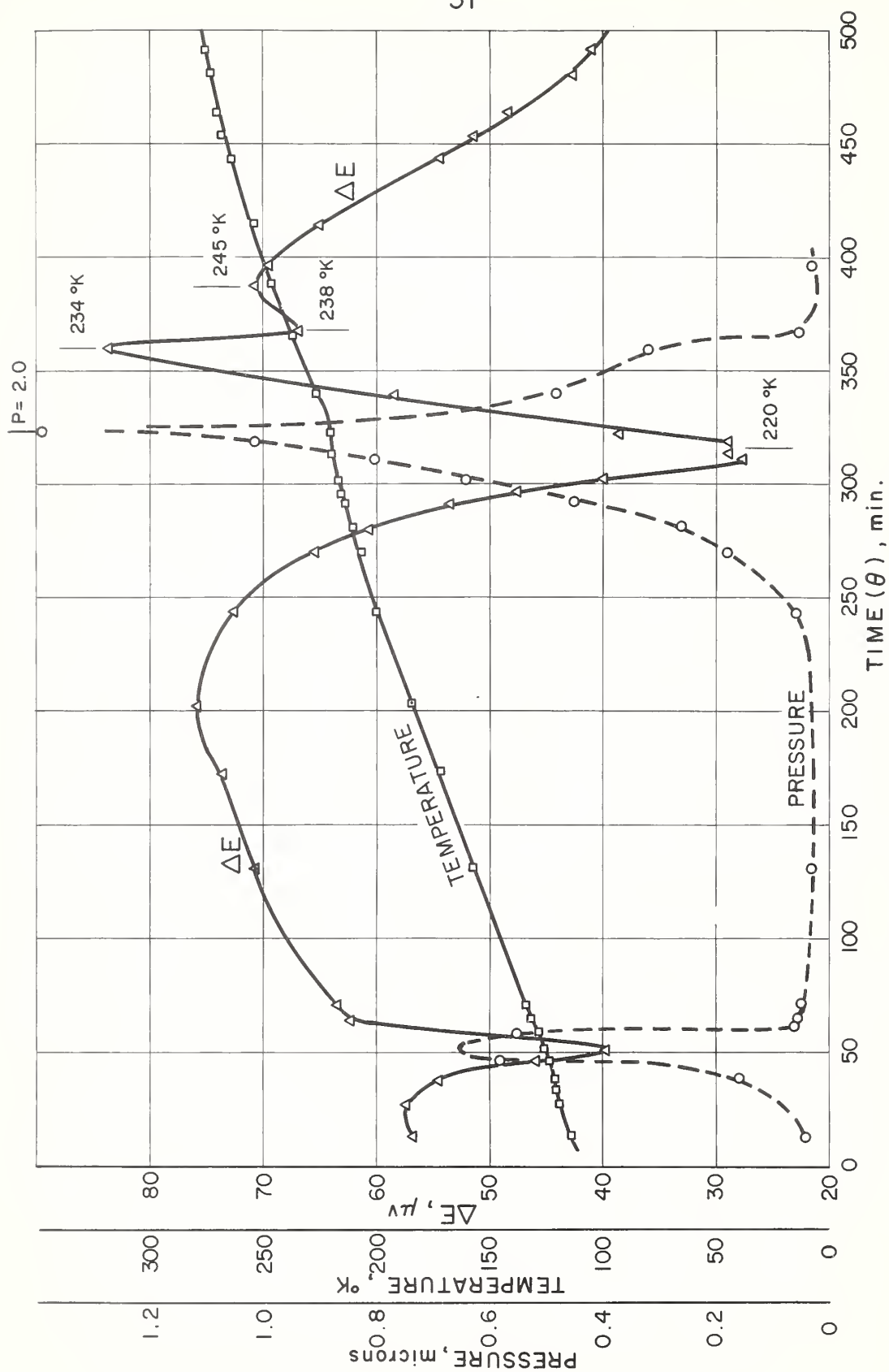
Figure 14. DTA Results, Compound V - 28B

Figure 15. DTA Results, Effects of Vacuum Environment, Compound I-12 D

properties of the dewar system used and is not considered to be an important defect at this time. If at some later date quantitative heat capacity and thermal conductivity information are desired, warming rates will have to be more accurately controlled.

Examination of the results indicates that the transition from the glassy state to the rubbery state gradually occurs over a temperature span of 9 to 20K°, depending on the material, and is accompanied by an increase in ΔE due to the increase in heat capacity. It was expected that this transition would take place in a more limited temperature interval, allowing an accurate definition of Tg similar to that indicated by heat capacity measurements. The range over which the transition occurs is noted on the graphs. An additional transition above Tg is noted in compound IV-29B, Figure 12, which is attributed to crystal melting. A crystal melting peak was noted about 25K° higher by Dannis[16], using a similar compound; however, melting started at a lower temperature in his tests.

4.4   Some Effects of Vacuum Environment in DTA

When the DTA tests were initiated it was assumed that a high vacuum environment around the sample would eliminate frost formation and facilitate temperature control. Test results have shown, however, that some effects in addition to the second order transitions and crystal melting influence ΔE. These unexpected effects are shown in Figure 15.

The three variables plotted against running time are sample temperature, ΔE, and pressure in the vacuum can. The unexpected phenomena take place over wide ranges of temperature, but peaks in the ΔE and P curves show 125°K and 220°K as the temperatures of the effects for compound I-12D. A natural rubber sample previously tested did not show a decided dip at any low temperature, but the large variation near 220°K was observed.

It is important to notice the large pressure rise in these two temperature regions, which occurred in spite of the fact that the system was continuously pumped by the oil diffusion pump at all times. At these points the temperature rise at the surface also stopped temporarily, indicating an endothermic process.

We do not understand these effects at this time, but we speculate that some of the compounding ingredients not chemically bonded in the

molecular structure are vaporizing in the presence of vacuum conditions. Another possibility is that contaminants in the vacuum space vaporize at these temperatures. In the tests to date it is quite possible that some condensibles were introduced during cooldown, and the author believes this to be the most likely explanation. However, a careful examination of this behavior will be pursued, since o-rings made from the materials may be recommended for high vacuum, low temperature static seals.

References

1. Weitzel, D. H., Robbins, R. F., Ludtke, P. R., Ohori, Y., Herring, R. N., Elastomeric Seals and Materials at Cryogenic Temperatures, Aeronautical Systems Division Technical Data Report 62-31.

2. Spencer, R. S., Boyer, R. F., Thermal Expansion and Second Order Transition Effects in High Polymers, Part III, J. App. Phys., 17 (1946).

3. Alfrey, T., Goldfinger, G., Mark, H., Apparent Second Order Transition Point of Polystyrene, J. Applied Physics, 14, (1943).

4. Boyer, R. F., Spencer, R. S., Thermal Expansion and Second Order Transition Effects in High Polymers, Part II, J. App. Phys., 16, 594 (1945).

5. Ehrenfest, P., Comm. Leiden, Suppl 75B (1933).

6. Powell, R. E., Rosevear, W. E., Eyring, H., J. App. Phys. 12, 669 (1941).

7. Fox, T. G., Florey, P. J., Second Order Transition Temperature and Related Properties of Polystyrene, Part I, J. App. Phys. 21, (1950).

8. Muller, A., Proc. Roy. Soc. A178, 227 (1941).

9. Williams, M. L., Landel, R. F., Ferry, J. D., J. Am. Chem. Soc., 77, 3701 (1955).

10. Tobolsky, I. V., Properties and Structure of Polymers, p. 83-88, John Wiley and Sons, Inc. (1960).

11. Bueche, F., J. Chem. Phys., 20, 1959 (1952).

12. Mendelkern, L., Martin, G. M., Quina, F. A. Jr., Glassy State Transitions of Poly (Chlorotrifluoroethylene), Poly (Vinylidene Fluoride) and Their Copolymers, J. Res. NBS, 58, No. 3, RP 2745 (1957).

5. Appendix. Compounding Recipes of ASD Materials

ASD No.	Polymer	Estimated Monomer Ratio	Recipe		Hardness (Shore A)
Group I					
I-8D	Vinylidene Fluoride & Perfluoropropylene ("Viton" A, Du Pont)	70/30	Polymer Magnesium Oxide Hexamethylene Diamine Carbamate M T Carbon Black Cure 20 min at 280 F Post cure 16 hr at 400 F	100 20 1.3 25	80
I-12A	Vinylidene Fluoride & Perfluoropropylene (Third Monomer Unknown) ("Viton" B, Du Pont)	Terpolymer	Additives ditto 8D Cure 20 min at 310 F Post cure 16 hr at 400 F		75
I-12B	Vinylidene Fluoride & Perfluoropropylene ("Viton" A-HV, Du Pont)	70/30	ditto		80
I-12C	Vinylidene Fluoride & Perfluoropropylene ("Fluorel", Minnesota Mining & Mfg.)	70/30	ditto		80
I-29F	Vinylidene Fluoride & Perfluoropropylene ("Viton" A, Du Pont)	70/30	Polymer Magnesium Oxide Hexamethylene Diamine Carbamate Cure 20 min at 310 F	100 20 1.3	65
I-12D	Vinylidene Fluoride & Monochlorotrifluoro-ethylene ("Kel F" 5500, Minnesota Mining & Mfg.)	50/50	Polymer Zinc Oxide "Hi Sil" Dibasic Lead Phosphite Benzoyl Peroxide Cure 20 min at 280 F Post cure 16 hr at 300 F	100 5 15 5 3	75

ASD No.	Polymer	Estimated Monomer Ratio	Recipe		Hardness (Shore A)
I-12E	Vinlyidene Fluoride & Monochlorotrifluoro-ethylene ("Kel F" 3700, Minnesota Mining & Mfg.)	70/30	Polymer Zinc Oxide E P Carbon Black Dibasic Lead Phosphite Hexamethylene Diamine Carbamate Cure 30 min at 310 F Post cure 13 hr at 300 F	100 5 10 5 1.3	80
I-25A	ditto	70/30	Polymer Dibasic Lead Phosphite Zinc Oxide Benzoyl Peroxide Silica Cure 20 min at 280 F	100 5 5 3 15	70
Group II					
II-21D	Butadiene & Styrene ("Synpol" 1000, Texas - U. S. Chem. Co.)	77/23	Polymer Zinc Oxide Benzothiazyl Disulfide Stearic Acid Sulfur Easy Process Channel Black Cure 50 min at 320 F	100 5 1.75 1.5 2 40	65
Group III					
III-12C	Isobutylene and Iso-prene (Butyl 035)	99/1	Polymer Zinc Oxide Stearic Acid Benzothiazyl Disulfide Tetra Methyl Thiuram Disulfide Sulfur High Abrasive Furnace Black Cure 30 min at 310 F	100 5 1 .5 1 2 50	70

ASD No.	Polymer	Estimated Monomer Ratio	Recipe		Hardness (Shore A)
III-12D	Isobutylene & Iso-prene (Butyl 325)	97.5/2.5	Polymer	100	75
			Zinc Oxide	5	
			Stearic Acid	1	
			Benzothiazyl Disulfide	.5	
			Tetra Methyl Thiuram Disulfide	1	
			Sulfur	2	
			High Abrasive Furnace Black	50	
			Cure 30 min at 310 F		
III-12E	ditto (Resin Cure)	97.5/2.5	Polymer	100	75
			Zinc Oxide	5	
			Stearic Acid	1	
			High Abrasive Furnace Black	50	
			Chlorinated Phenolic Resin	12	
			Cure 30 min at 310 F		
III-12A	Isobutylene & Iso-prene (Brominated) ("Hycar" 2202, B. F. Goodrich Chem. Co.)	---	Polymer	100	80
			Zinc Oxide	5	
			Stearic Acid	3	
			Benzothiazyl Disulfide	.4	
			Tetra Methyl Thiuram Disulfide	.8	
			Sulfur	2	
			Easy Process Channel Black	50	
			Cure 30 min at 310 F		
III-12B	Isobutylene & Iso-prene (Chlorinated, 1%) (HT-66, Enjay Chem. Co.)	97/2/1	Polymer	100	70
			Zinc Oxide	5	
			Stearic Acid	1	
			Benzothiazyl Disulfide	.5	
			Tetra Methyl Thiuram Disulfide	1	
			Sulfur	2	
			High Abrasive Furnace Black	50	

ASD No.	Polymer	Estimated Monomer Ratio	Recipe		Hardness (Shore A)
Group IV					
IV-8A	Natural Rubber (Smoked Sheet)		Polymer	100	65
			Stearic Acid	3	
			Zinc Oxide	5	
			N-Cyclohexyl-2-Benzothiazole Sulfenamide	.6	
			Sulfur	2.75	
			High Abrasive Furnace Black	50	
			Polymerized trimethyldi-hydroquinoline (Resin D)	1	
			Cure 15 min at 310 F		
IV-8B	Chloroprene (Neoprene, Du Pont)		Polymer	100	85
			Stearic Acid	5	
			Zinc Oxide	5	
			Magnesium Oxide	4	
			High Modulus Furnace Black	50	
			Na 22	.5	
			Cure 20 min at 310 F		
IV-29B	Cis 4 Polybutadiene		Polymer	100	70
			Zinc Oxide	5	
			Stearic Acid	.5	
			Sulfur	2.5	
			High Abrasive Furnace Black	50	
			Cure 30 min at 310 F		
IV-29C	Ethylene and Propylene (EPR-40)		Polymer	100	60
			Stearic Acid	1	
			Sulfur	.8	
			High Abrasive Furnace Black	50	
			Dicumyl Peroxide	4	
			Cure 20 min at 310 F		

THE NATIONAL BUREAU OF STANDARDS

The scope of activities of the National Bureau of Standards at its major laboratories in Washington, D.C., and Boulder, Colorado, is suggested in the following listing of the divisions and sections engaged in technical work. In general, each section carries out specialized research, development, and engineering in the field indicated by its title. A brief description of the activities, and of the resultant publications, appears on the inside of the front cover.

WASHINGTON, D.C.

Electricity. Resistance and Reactance. Electrochemistry. Electrical Instruments. Magnetic Measurements. Dielectrics. High Voltage.

Metrology. Photometry and Colorimetry. Refractometry. Photographic Research. Length. Engineering Metrology. Mass and Scale. Volumetry and Densimetry.

Heat. Temperature Physics. Heat Measurements. Cryogenic Physics. Equation of State. Statistical Physics.

Radiation Physics. X-ray. Radioactivity. Radiation Theory. High Energy Radiation. Radiological Equipment. Nucleonic Instrumentation. Neutron Physics.

Analytical and Inorganic Chemistry. Pure Substances. Spectrochemistry. Solution Chemistry. Standard Reference Materials. Applied Analytical Research.

Mechanics. Sound. Pressure and Vacuum. Fluid Mechanics. Engineering Mechanics. Rheology. Combustion Controls.

Organic and Fibrous Materials. Rubber. Textiles. Paper. Leather. Testing and Specifications. Polymer Structure. Plastics. Dental Research.

Metallurgy. Thermal Metallurgy. Chemical Metallurgy. Mechanical Metallurgy. Corrosion. Metal Physics. Electrolysis and Metal Deposition.

Mineral Products. Engineering Ceramics. Glass. Refractories. Enameled Metals. Crystal Growth. Physical Properties. Constitution and Microstructure.

Building Research. Structural Engineering. Fire Research. Mechanical Systems. Organic Building Materials. Codes and Safety Standards. Heat Transfer. Inorganic Building Materials.

Applied Mathematics. Numerical Analysis. Computation. Statistical Engineering. Mathematical Physics. Operations Research.

Data Processing Systems. Components and Techniques. Computer Technology. Measurements Automation. Engineering Applications. Systems Analysis.

Atomic Physics. Spectroscopy. Infrared Spectroscopy. Solid State Physics. Electron Physics. Atomic Physics.

Instrumentation. Engineering Electronics. Electron Devices. Electronic Instrumentation. Mechanical Instruments. Basic Instrumentation.

Physical Chemistry. Thermochemistry. Surface Chemistry. Organic Chemistry. Molecular Spectroscopy. Molecular Kinetics. Mass Spectrometry.

Office of Weights and Measures.

BOULDER, COLO.

Cryogenic Engineering. Cryogenic Equipment. Cryogenic Processes. Properties of Materials. Cryogenic Technical Services.

Ionosphere Research and Propagation. Low Frequency and Very Low Frequency Research. Ionosphere Research. Prediction Services. Sun-Earth Relationships. Field Engineering. Radio Warning Services. Vertical Soundings Research.

Radio Propagation Engineering. Data Reduction Instrumentation. Radio Noise. Tropospheric Measurements. Tropospheric Analysis. Propagation-Terrain Effects. Radio-Meteorology. Lower Atmosphere Physics.

Radio Standards. High Frequency Electrical Standards. Radio Broadcast Service. Radio and Microwave Materials. Atomic Frequency and Time Interval Standards. Electronic Calibration Center. Millimeter-Wave Research. Microwave Circuit Standards.

Radio Systems. Applied Electromagnetic Theory. High Frequency and Very High Frequency Research. Modulation Research. Antenna Research. Navigation Systems.

Upper Atmosphere and Space Physics. Upper Atmosphere and Plasma Physics. Ionosphere and Exosphere Scatter. Airglow and Aurora. Ionospheric Radio Astronomy.